Les Cahiers du GERAD ISSN: 0711–2440

A novel sequential Benders-semidefinite framework with dual feasible proxy for multi-stage transmission expansion planning with contingencies

E. Fathipasandideh, H. Suprême, H. Dagdougui, C. Audet, D. Asber

G–2025–83

December 2025

La publication de ces rapports de recherche est rendue possible grâce au soutien de HEC Montréal, Polytechnique Montréal, Université McGill, Université du Québec à Montréal, ainsi que du Fonds de recherche du Québec – Nature et technologies.

Dépôt légal – Bibliothèque et Archives nationales du Québec, 2025
– Bibliothèque et Archives Canada, 2025

The publication of these research reports is made possible thanks to the support of HEC Montréal, Polytechnique Montréal, McGill University, Université du Québec à Montréal, as well as the Fonds de recherche du Québec – Nature et technologies.

Legal deposit – Bibliothèque et Archives nationales du Québec, 2025
– Library and Archives Canada, 2025

GERAD HEC Montréal
3000, chemin de la Côte-Sainte-Catherine
Montréal (Québec) Canada H3T 2A7

Tél. : 514 340-6053
Téléc. : 514 340-5665
info@gerad.ca
www.gerad.ca

A novel sequential Benders-semidefinite framework with dual feasible proxy for multi-stage transmission expansion planning with contingencies

Elmira Fathipasandideh [a, b]

Hussein Suprême [a, c]

Hanane Dagdougui [a, b]

Charles Audet [a, b]

Dalal Asber [a]

[a] *Département de mathématiques et de génie industriel, Polytechnique Montréal, Montréal, (Qc), Canada, H3T 1J4*

[b] *GERAD, Montréal (Qc), Canada, H3T 1J4*

[c] *Hydro-Québec Research Institute (IREQ), Hydro-Québec, Varennes (Qc), Canada, J3X 1S1*

elmira.fathipasandideh@polymtl.ca
hanane.dagdougui@polymtl.ca
charles.audet@polymtl.ca
supreme.hussein2@hydroquebec.com

December 2025
Les Cahiers du GERAD
G–2025–83

Abstract : This paper presents a transmission expansion planning framework that couples Benders decomposition with an operational layer based on a semidefinite programming (SDP) relaxation of the alternating-current optimal power flow (AC-OPF). The mixed-integer linear programming (MILP) master problem selects line and reactive-power investments across stages and operating conditions, while SDP subproblems evaluate operating cost. To accelerate convergence, we introduce a learned dual-feasible proxy that provides certified dual lower bounds, prioritizes subproblems with greatest impact, and warm-starts the remaining SDP solves. Optimality cuts are always derived from exact dual solutions, preserving convergence guarantees. Numerical experiments on IEEE 24-, 118-, and 300-bus systems demonstrate significant reductions in runtime and SDP evaluations, tight primal–dual gaps, and full AC feasibility without load shedding. The results show that a "Benders-first, SDP-second" strategy, enhanced with dual-feasible proxies, offers a practical and scalable solution for secure multistage planning in realistic power networks.

Keywords : Benders decomposition; design optimization; optimal power flow calculations; semidefinite programming; transmission network expansion planning

1 Introduction

Transmission networks form the backbone of modern power systems, ensuring the reliable and secure delivery of electricity from generation sites to consumption centers. However, growing demand, aging infrastructure, market restructuring, climate changes, and accelerating the integration of renewable energy sources have increased the complexity of long-term transmission planning [17, 16]. To address these challenges, transmission operators must rely on advanced optimization techniques to guide strategic investment decisions. Transmission network expansion planning (TNEP) identifies cost-effective additions of equipment to satisfy future needs and strengthen system resilience. Crucially, these investments must remain robust under both normal operating conditions and contingency scenarios. Complementing TNEP, reactive power planning (RPP) ensures voltage stability by optimally placing and sizing reactive power resources [19]. Inadequate reactive support can precipitate voltage collapse and large-scale outages, making RPP an indispensable counterpart in long-term planning [18].

Despite their interdependence, TNEP and RPP are often treated separately due to their inherent complexity [9]. Both problems are typically formulated as large-scale mixed-integer nonlinear programs (MINLPs) with nonconvex AC power flow constraints, posing significant computational challenges, especially for large-scale systems and multistage planning horizons. A further practical requirement in TNEP is the incorporation of *N–1* security constraints, which guarantees system resiliency under any single component failure. Ignoring such contingencies can result in investment plans that are economically efficient but operationally fragile [11]. Explicit modeling of *N–1* security ensures that expansion decisions both minimize costs and enhance robustness.

Various solution methodologies have been explored for TNEP and RPP. Heuristic methods offer fast and simple solutions but often sacrifice optimality [3]. Benders decomposition separates the problem into a master investment model and an operational subproblem [4]; however, its classical form assumes convex subproblems, an assumption violated in power systems, leading to weak or invalid cuts [2]. Metaheuristics can scale well, but typically rely on simplified models [1, 10], which may overlook nonconvex phenomena and result in infeasible or suboptimal solutions.

Multistage planning has also been incorporated into TNEP [15] by replicating decisions and constraints across stages and accounting for intertemporal couplings in the objective. While conceptually straightforward, this substantially enlarges the problem. To mitigate such limitation, two strategies have proved to be effective: 1) decomposition techniques and 2) convex relaxation methods. Decomposition partitions large models into tractable subproblems [12]. Convex relaxations transform nonconvex constraints into convex forms; among these, semidefinite programming (SDP) provides strong lower bounds and near-global solutions for AC power flow [8]. SDP has therefore become a valuable tool for nonconvex power system optimization, reformulating difficult AC models into convex counterparts [20]. Notable advances include conic programming for TNEP [7] and mixed-integer SDP branch-and-cut for AC-TNEP [6]. Nevertheless, most studies either focus on single-stage planning or treat TNEP and RPP separately, overlooking their interdependence and the complexities of evolving conditions.

In our prior work [5], we propose a sequential framework combining Benders decomposition with SDP relaxation, preserving AC fidelity while improving scalability compared to monolithic SDP formulations. Nonetheless, two key limitations remained: the absence of explicit *N–1* security modeling and the high cost of repeatedly solving SDP subproblems. Although SDP relaxations yield strong bounds, their computational burden can dominate end-to-end runtime. In a Benders loop, each iteration entails multiple SDP solves, and the cost grows rapidly with network size, the number of stages, and especially the contingency set. Under *N–1* security constraints, every single-element outage introduces additional evaluations. Thus, while SDP promotes accuracy and robustness, it can impede the scalability of secure multistage TNEP.

To overcome this bottleneck, we introduce a dual-feasible proxy for the SDP subproblems. This proxy constructs dual points that are feasible by design-enforcing non-negativity for inequality duals and projecting conic blocks onto the positive semi-definite cone, thereby providing certified lower bounds and effective warm starts for the SDP solver. Inspired by recent developments in dual conic proxies for AC-OPF [14], our method adapts these ideas to the Benders-SDP architecture for secure, multistage TNEP with contingencies. Integrating the proxy into the decomposition loop significantly reduces wall-clock time while preserving solution quality and correctness, enabling scalable and robust transmission expansion planning.

The main contributions of this work are:

1. A unified multistage TNEP+RPP framework coupling a MILP master problem with SDP-relaxed AC-OPF subproblems, preserving AC fidelity while scaling via decomposition.
2. Explicit incorporation of *N–1* security constraints within the sequential Benders–SDP formulation to guarantee feasibility under single contingencies.
3. The implementation of a *dual-feasible proxy* that supplies certified dual bounds and warm starts, reducing subproblem solve time without compromising outer-loop correctness.
4. Numerical evaluation on benchmark networks demonstrating improved runtime and solution quality versus MILP-based and unstrengthened Benders baselines.

2 Problem formulation

2.1 Multistage AC TNEP with N–1 security constraints

We address a multistage TNEP problem with reactive power support under explicit $N-1$ security constraints. The planning horizon is divided into stages $\mathcal{T}$, and each stage $t \in \mathcal{T}$ considers a set of operating conditions Ω_t comprising the base case and all single-contingency outages. Investment decisions $x \in \{0,1\}^{|\mathcal{C}|}$ encode candidate line additions and, when applicable, discrete reactive devices.[1]

Given x, each (t, ω) induces a network topology and parameters (thermal limits, admittances, generator sets) and defines a convex recourse cost $\theta_{t,\omega}(x)$ via a SDP relaxation of AC–OPF. The overall objective minimizes the discounted sum of investment and operating costs:

$$\min_{x} \ \mathrm{CapEx}(x) + \sum_{t\in\mathcal{T}} \sum_{\omega\in\Omega_t} \pi_{t,\omega}\, \theta_{t,\omega}(x), \tag{1}$$

where $\pi_{t,\omega} \geq 0$ are scenario weights. Stagewise budget and buildability constraints are enforced in $\mathcal{X}$, and security validation spans all Ω_t.

Unlike classical approaches that either ignore security constraints or treat TNEP and RPP separately, our framework integrates both in a unified multistage model while preserving AC fidelity through SDP relaxations. To ensure scalability and robustness, we propose two main contributions: a dual-feasible proxy that accelerates Benders decomposition by generating valid inexact cuts and warm starts, and Pareto-optimal cut strengthening combined with adaptive *N–1* screening to reduce iterations and computational burden. This combination enables secure, high-fidelity planning at realistic network sizes, meeting the computational and reliability standards required for future power systems.

2.2 Decomposition and operational subproblem

We adopt a generalized Benders decomposition (GBD) framework, which separates discrete investment decisions in the master problem from operational costs evaluated under each stage and contingency in convex subproblems. The master introduces epigraph variables $\theta_{t,\omega}$ and progressively enforces operational feasibility through Benders cuts that iteratively link $\theta_{t,\omega}$ to the investment vector x.

[1] For readability, all discrete investments are collected into x. If needed, x can be partitioned into line counts n and device placements z.

$$\begin{aligned} \min_{x,\theta} \quad & \mathrm{CapEx}(x) + \sum_{t,\omega} \pi_{t,\omega}\, \theta_{t,\omega} \\ \text{s.t.} \quad & x \in \mathcal{X}, \quad \theta_{t,\omega} \in \mathbb{R}. \end{aligned} \tag{2}$$

At iteration k, each active subproblem returns a value $\beta_{t,\omega}(x^k)$ and a subgradient $g_{t,\omega}(x^k)$, yielding multi-cuts:

$$\theta_{t,\omega} \geq \beta_{t,\omega}(x^k) + g_{t,\omega}(x^k)^\top (x - x^k), \quad \forall (t,\omega) \text{ active.} \tag{3}$$

Each subproblem is formulated as a semidefinite relaxation of AC–OPF:

$$\begin{aligned} \theta_{t,\omega}(x^k) = \min_{W,p,q,\ell} \quad & c^\top p + d^\top q + \varepsilon\, \mathrm{tr}(W) \\ \text{s.t.} \quad & \mathcal{A}(W,p,q,\ell;\, x^k, t, \omega) = 0, \\ & \mathcal{B}(W,p,q,\ell;\, x^k, t, \omega) \leq 0, \\ & W \succeq 0, \;\; \ell \in \mathcal{K}. \end{aligned} \tag{4}$$

where $\mathcal{A}$ enforces power balance, and $\mathcal{B}$ captures voltage limits, thermal constraints and SDP constraints.

A small $\varepsilon \in \{0, 10^{-5}, 10^{-4}\}$ promotes low rank without affecting investment decisions. The dual solution of (4) provides $\beta_{t,\omega}(x^k)$ and $g_{t,\omega}(x^k)$ for cut generation. This decomposition preserves AC fidelity while enabling scalability, forming the foundation for the proposed enhancements.

3 Proposed algorithmic framework

Algorithm 1 Sequential Benders–SDP Framework with DFP and MW Strengthening.

Initialize: x^0, incumbent $\hat{x} \leftarrow x^0$, cut pool $\mathcal{C} \leftarrow \emptyset$, screened sets $\{\Omega_t^0\}$.
for $k = 0, 1, 2, \ldots$ **do**
    Solve master problem (2) to get x^k and LB^k.
    Perform adaptive security screening to update $\{\Omega_t^k\}$.
    for all $(t, o) \in \Omega_t^k$ **in parallel do**
        if $k \bmod r \neq 0$ **then**
            Generate DFP-based inexact (3).
        else
            Solve SDP subproblem to optimality (4).
            Apply MW strengthening (6).
            Generate Pareto-optimal cut.
        end if
    end for
    Update $\mathcal{C}$ with violated cuts.
    if Primal bound evaluation **then**
        Update $\hat{x}$ and UB^k
    end if
    if $UB^k - LB^k \leq 0.1\% \wedge OpSecu$ **then**
        break
    end if
end for

3.1 Sequential algorithm description

As shown in Algorithm 1, each iteration begins by solving the master problem to update the investment plan and lower bound. A fast screening procedure identifies critical contingencies, updating the active set of operating conditions. For each contingency, feasibility cuts are generated in parallel: most iterations use inexact cuts derived from DFP, while periodic refreshes invoke exact SDP solves enhanced by Pareto-optimal Magnanti–Wong strengthening. The cut pool and incumbent are updated based on recourse improvements. The process terminates once the optimality gap is sufficiently small and full AC power flow N–1 validation confirms operational security (OpSecu). The main steps of the algorithm are detailed below.

3.2 Dual–Feasible Proxy (DFP) for inexact Benders cuts

Goal. For each active stage/operating condition (t, o), the objective is to obtain a *cheap* yet *valid* lower supporting hyperplane of the SDP value function $\theta_{t,o}(\cdot)$ at the current investment x^k, without fully solving the slave SDP (4) to optimality.

Key idea. Any *dual-feasible* point of the slave SDP yields a valid lower bound and hence a valid Benders cut. The DFP method constructs such a point quickly by (i) generating a raw dual estimate and (ii) projecting onto the dual-feasible set. This generates an *inexact* cut that is conservative (never overestimates $\theta_{t,o}$) and significantly cheaper than an exact cut.

Raw dual estimate. A preliminary dual tuple $\widehat{\pi} = (\widehat{\lambda}, \widehat{\mu}, \widehat{\nu}, \widehat{S}, \ldots)$ is obtained via:

1. Interior-point method (IPM) snapshot: Run K iterations (e.g., $K \in \{3, 5\}$) of the IPM on (4) and extract the current duals;
2. Learned initializer (optional): Predict $\widehat{\pi}$ from features (x^k, t, o) using a lightweight neural network.

Feasibility repair. Let $\mathcal{D}_{t,o}$ denote the dual feasible set of (4). We map $\widehat{\pi}$ to a *dual-feasible* $\pi \in \mathcal{D}_{t,o}$ via closed-form projections:

1. Linear/SOC inequality duals: project to the nonnegative cone: $\lambda \leftarrow \max\{0, \widehat{\lambda}\}$, etc.; for SOC blocks use standard Euclidean cone projection.
2. PSD dual block: symmetrize and shift to the PSD cone:
$$S \leftarrow \tfrac{1}{2}(\widehat{S} + \widehat{S}^\top) - \min\big\{0, \lambda_{\min}\big(\tfrac{1}{2}(\widehat{S} + \widehat{S}^\top)\big)\big\}\, I,$$
so that $S \succeq 0$ holds by construction.

After repair, π satisfies all dual conic and sign constraints and is therefore dual-feasible.

Inexact cut construction. Evaluate the dual objective $\beta_{t,o}(x^k)$ at π and assemble the master-space subgradient $g_{t,o}(x^k)$ from the repaired dual components (thermal, voltage, generator bounds, etc.). Add the *inexact* but valid multi-cut
$$\theta_{t,o} \;\geq\; \beta_{t,o}(x^k) \;+\; g_{t,o}(x^k)^\top (x - x^k). \tag{5}$$
We accept a cut only if its violation at x^k exceeds a small threshold (e.g., 10^{-5}) to avoid numerically flat planes.

Scheduling and guarantees. DFP cuts are added in *most* outer iterations; every r iterations (e.g., r=3) we solve the slave (4) to optimality and (optionally) apply MW strengthening to refresh tightness. Because DFP cuts are dual-feasible, the master problem's lower bound is nondecreasing and conservative. Periodic exact solves ensure the cut family approaches the true recourse function, yielding finite convergence under standard convex GBD assumptions.

Warm-starting benefit. The repaired dual π also serves as an excellent warm start for the next exact slave solve, typically reducing IPM iterations and wall-time.

3.3 Pareto-optimal cut strengthening via Magnanti–Wong

Exact cuts generated at x^k are valid but often weak away from that point. To strengthen them, we apply the Magnanti–Wong procedure, which selects a Pareto-optimal dual solution—optimal for the subproblem (4) at x^k and normalized such that $\|g_{t,o}(x^k)\|_1 = 1$—that maximizes separation at a reference point $\bar{x} = \alpha x^k + (1-\alpha)\hat{x}$, with $\alpha \in (0,1)$ and incumbent $\hat{x}$.

This leads to the auxiliary problem:

$$\max_{\text{dual feasible}} \quad \beta_{t,o}(x^k) + g_{t,o}(x^k)^\top (\bar{x} - x^k). \tag{6}$$

By "dual feasible" we mean a set of multipliers u for the SDP slave at (t,o) and anchor x^k that satisfies all dual constraints of the subproblems. Under dual feasibility, the Lagrangian lower bound

$$\sigma_{t,o} \;\geq\; \inf_{X_{t,o}} \left\{ f_2(X_{t,o},\cdot) \;+\; u^\top G_2(X_{t,o},\cdot) \right\}$$

is valid, which is precisely the quantity used to build the Benders optimality cut.

The resulting cut improves separation near $\bar{x}$ and accelerates convergence. In our implementation, Magnanti–Wong cuts are refreshed every r outer iterations, with $r = 3$ by default.

3.4 Adaptive N–1 screening and validation

Modeling N–1. Let Ω_t be the set of operating conditions at stage t, consisting of the base case and all single-element outages (lines/transformers, and optionally generators). Each $\omega \subseteq \Omega_t$ modifies the network by enforcing an outage mask on the admittance and limits, e.g.,

$$Y^{(t,\omega)} = Y^{(t)} \circ M^{(\omega)}, I^{(t,\omega)}_{\ell,\max} = \begin{cases} 0 & \text{if line } \ell \nsubseteq \omega, \\ I^{(t)}_{\ell,\max} & \text{otherwise,} \end{cases}$$

and the slave (4) is solved with $(Y^{(t,\omega)}, I^{(t,\omega)}_{\ell,\max})$ and the topology induced by x^k (cumulative builds up to stage t). Thus, for every (t,ω), the recourse value $\theta_{t,\omega}(x)$ captures the *secured* operating cost under that contingency.

Why screening is needed? Enumerating all N–1 scenarios at every iteration is prohibitive for large networks. Instead, we maintain a manageable *active* subset $\Omega_t^k \subseteq \Omega_t$ that is updated as the master solution x^k evolves.

Adaptive screening loop. After each master solve:

1. **Fast check on full list.** Using the current investment x^k, run a quick DC or SOC security assessment on *all* single outages in Ω_t; compute a violation score (e.g., max line overload or voltage deviation).
2. **Promote violators.** Add the top-M new violators (largest scores not already in Ω_t^k) to the active set to obtain Ω_t^{k+1}.
3. **Solve SDPs only for Ω_t^{k+1}.** For new members use DFP cuts first; on refresh iterations solve to optimality and (optionally) apply MW strengthening.

This strategy keeps the per-iteration cost low while focusing effort where the current plan is most stressed.

Exactness at termination. At convergence, we perform a *full* AC power-flow validation of the incumbent plan against the *entire* N–1 set Ω_t. If any new violator appears, it is added to Ω_t^k and the loop continues, ensuring that the final design is truly N–1 secure.

4 Computational experiments

4.1 Test systems and setup

We evaluate the framework on the RTS–24, IEEE 118-bus, and IEEE 300-bus systems [13]. All systems are analyzed over a 15-year planning horizon divided into three 5-year stages. The operational horizon spans years 5 to 10. An annual discount rate of 10% and a load factor of 0.6 are used. The time base is set to 8760 hours per year, with one hour discounted for each contingency. Shunt reactive power support is modeled through VAr sources with fixed susceptance of 0.2 p.u. and unit cost of 0.05 million USD. Voltage magnitudes are constrained between 0.95 and 1.05 p.u. in both normal operation and contingency conditions. To enhance numerical conditioning, a small resistance of 10^{-5} p.u. is added to each transformer. All experiments are run on a 3.40 GHz Intel Core i7–4770 processor with 16 GB of RAM. CPU thread counts are limited to prevent oversubscription. SDP subproblems are solved using MOSEK v8.1.0.56 with default settings, chordal decomposition, and solver tolerances of 10^{-6}. The master problem is modeled as a MILP and solved using Gurobi. Contingency screening is performed using fast DC or SOC relaxations, followed by full AC power flow validation. The dual feasibility proxy (DFP) is implemented in Python 3.10 using PyTorch 2.0 and trained with the Adam optimizer. Training is performed on GPU when available, while inference during the Benders loop runs on CPU. All final expansion plans are validated through full AC power flow simulations under the base case and complete N–1 contingency set to ensure physical feasibility and zero load shedding.

4.2 Algorithm performance metrics

Performance results for the three algorithmic variants are summarized. Runtime and iteration counts in Figure 1 show a clear trend: RTS–24, IEEE–118, and IEEE–300 exhibit substantial reductions in computation time when moving from the baseline BDSDP to the DFP-enhanced variants. For example, IEEE–300 decreases from 231.4 minutes to 38.9 minutes, while iterations drop from 34 to 11. Similar patterns occur for the smaller systems, confirming that the acceleration scales with problem size.

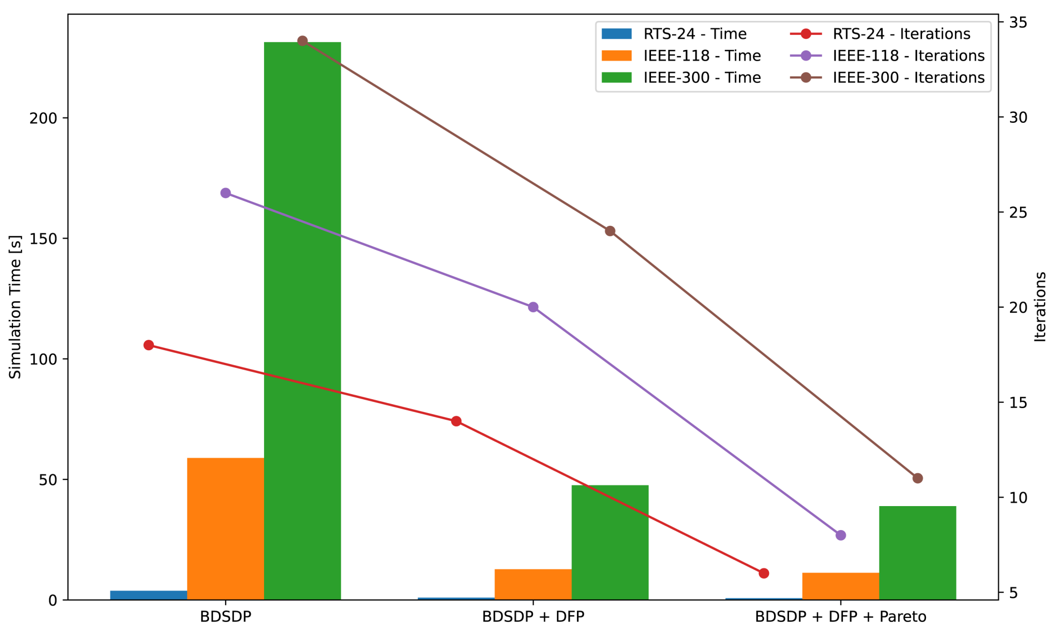

Figure 1: Simulation time and iterations per method and system.

Here, SDP_e denotes exact semidefinite slave solves (the full SDP solved to tolerance), while SDP_i denotes inexact but dual-feasible proxy solves: the proxy completes the SDP dual so that all dual equalities and PSD conditions hold, yielding a valid dual objective and therefore valid Benders cuts. In other words, SDP_i are not violations—they are cheaper, dual-feasible evaluations that safely replace many exact SDPs. The distribution of exact and inexact solves in Table 1 highlights the source of the gains: exact solves (SDP_e) drop sharply—for example, from 548 to 172 on IEEE–300—while inexact solves (SDP_i) rise accordingly. This shift shows that most of the heavy computation is replaced by fast, dual-feasible proxy evaluations without compromising feasibility.

Table 1: SDP constraint violations.

System	Method	SDP_e	SDP_i
RTS–24	BDSDP	18	0
	BDSDP + DFP	0	41
	BDSDP + DFP + Pareto	0	52
IEEE–118	BDSDP	209	0
	BDSDP + DFP	116	85
	BDSDP + DFP + Pareto	77	116
IEEE–300	BDSDP	548	0
	BDSDP + DFP	296	224
	BDSDP + DFP + Pareto	172	322

Solution quality remains consistent across all cases, as illustrated in Figure 2. Rank-1 recovery rates improve steadily, reaching 80.6% on IEEE–300, while the final master gap stays within a narrow 5–12% range. These results confirm that the acceleration strategies maintain physical feasibility and optimality characteristics, even under aggressive reductions in exact computations.

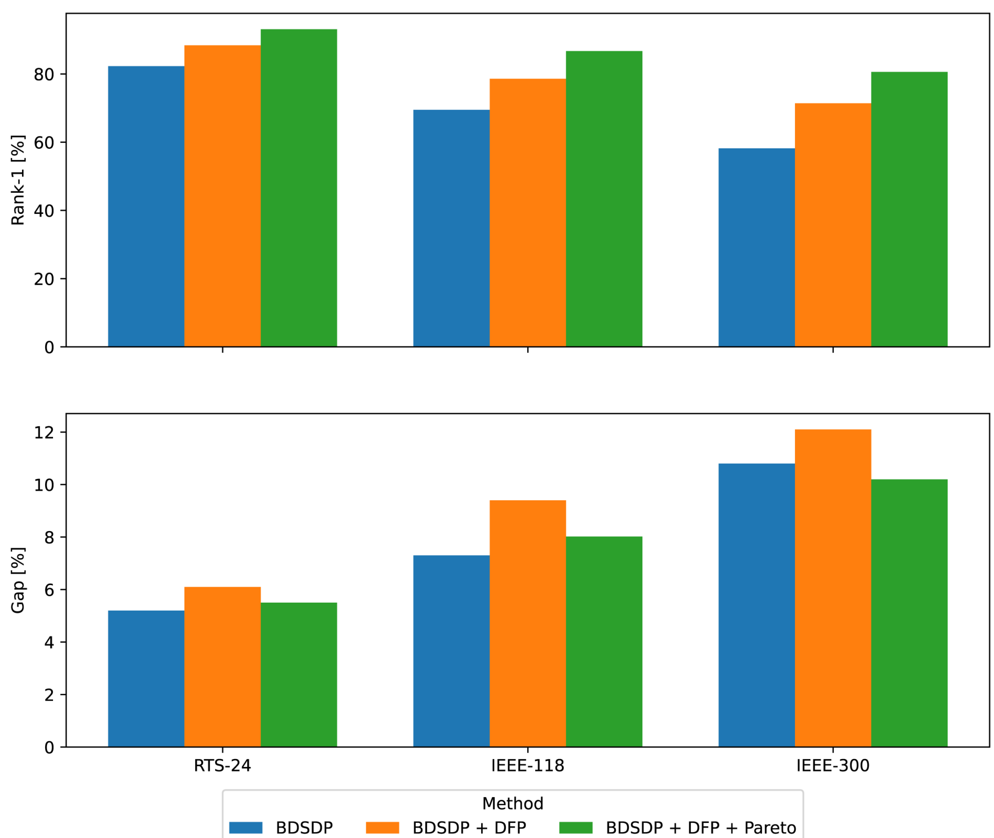

Figure 2: Comparison of rank-1 feasibility and optimality gap.

The behavior of the dual lower bounds is illustrated in Figure 3, which compares the true SDP-based bounds with those obtained from the DFP proxy across all systems. The curves show that proxy-based bounds track the true bounds closely throughout the master iterations, even for large-scale cases like IEEE–300. For RTS–24 and IEEE–118, the gap between proxy and true bounds is negligible, while for IEEE–300 the proxy remains within a tight margin of the exact bound. This alignment confirms that the inexact projections provide reliable dual information, enabling valid Benders cuts without compromising convergence. The consistency across all systems explains why the proposed acceleration achieves significant runtime reductions while maintaining solution quality.

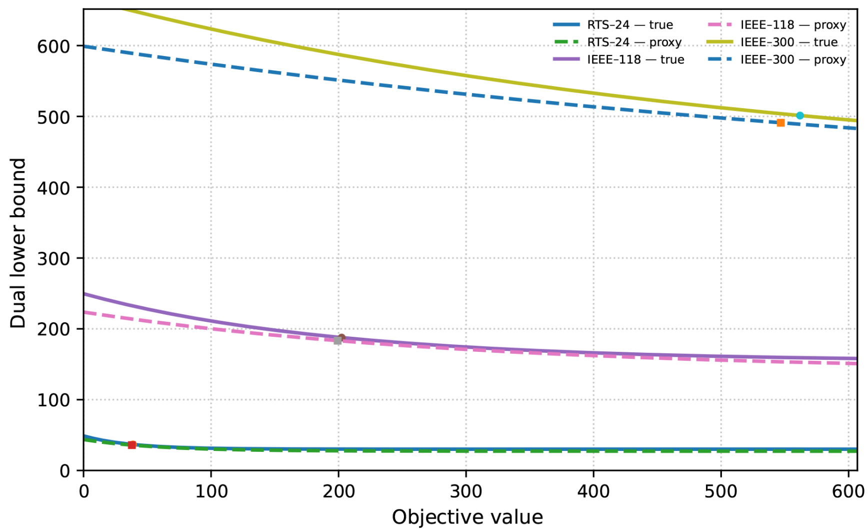

Figure 3: True dual vs. proxy (dashed) for RTS–24, IEEE–118, IEEE–300.

Overall, the performance metrics demonstrate that the proposed enhancements significantly reduce runtime and iteration counts while preserving solution quality, making the approach particularly effective for large-scale systems.

4.3 Planning results and validation

Table 2 summarizes the stage-wise investment decisions for each test system. The proposed configurations allocate reinforcements progressively, with early stages focusing on critical corridors and later stages adding redundancy and reactive support. This is reflected in the quantity and timing of infrastructure deployment.

Across all systems, over 45% of line and shunt installations are concentrated in Stage 1, highlighting a strategic emphasis on early congestion relief and voltage support. RTS–24 deploys 4 lines and 6 shunts in total, with 56% of devices installed in Stage 1. IEEE–118 adds 15 lines and 25 shunts, 48% of which are placed in the first stage. IEEE–300 sees the largest deployment, with 24 lines and 38 shunts overall, and 47% installed in Stage 1. The total capital expenditure (CAPEX) scales with system size, from \$7.9M for RTS–24 to \$103.6M for IEEE–300. This phased approach prioritizes early reinforcement, followed by targeted upgrades to ensure operational security and reactive support under contingencies.

The CAPEX trends in Table 3 reveal a deliberate front-loading of investments, with Stage 1 absorbing nearly half of the total budget across all systems. This early concentration enables foundational upgrades, while Stages 2 and 3 show a consistent decline in spending—between 32% and 45%—as reinforcements become more targeted. The cumulative growth from Stage 1 to Stage 2 exceeds 65% for IEEE–118 and IEEE–300, indicating a substantial mid-horizon expansion before tapering off. The result is a staged plan that builds the bulk of capacity up front and finishes with focused adjustments rather than broad expansions.

Table 2: Stage-wise investments for the proposed configuration.

System	**Stage 1**		**Stage 2**		**Stage 3**		**CAPEX** (M$)
	Lines	Shunts	Lines	Shunts	Lines	Shunts	
RTS–24	(1–2), (5–10)	7, 14, 18	(14–16)	9, 20	(16–19)	15	**7.90**
IEEE–118	(1–2), (1–3), (4–5), (5–6), (8–9), (9–10), (11–12)	7, 14, 19, 27, 33, 38, 45, 52, 66, 74, 85, 92	(12–14), (13–15), (14–15), (12–16), (15–17)	12, 26, 41, 57, 88, 95, 102, 109	(16–17), (17–18), (18–19)	11, 36, 54, 81, 118	**67.10**
IEEE–300	(1–5), (2–6), (2–8), (3–7), (3–19), (3–150), (5–9), (7–12), (8–11), (8–14), (9–11), (11–13)	15, 22, 31, 44, 56, 63, 79, 101, 119, 138, 152, 177, 201, 224, 249, 272, 289, 300	(12–21), (13–20), (14–15), (15–37), (15–89), (19–21), (20–22), (23–25)	18, 29, 47, 68, 97, 123, 166, 198, 233, 261, 287, 299	(24–319), (25–26), (26–27), (33–38)	35, 76, 149, 185, 230, 276, 295, 300	**103.60**

Table 3: Per-stage CAPEX and growth.

System	Stage	CAPEX [M$]	Δ_{stage} [%]	Cum. [M$]	Δ_{cum} [%]
RTS–24	1	4.20	–	4.20	–
	2	2.30	−45.24	6.50	+54.76
	3	1.40	−39.13	7.90	+21.54
IEEE–118	1	32.50	–	32.50	–
	2	21.70	−33.23	54.20	+66.77
	3	12.90	−40.55	67.10	+23.80
IEEE–300	1	49.80	–	49.80	–
	2	33.70	−32.33	83.50	+67.67
	3	20.10	−40.36	103.60	+24.07

Feasibility under AC N–1 conditions is confirmed in Table 4. Across all systems, voltage deviations remain below 0.025 p.u., line loadings stay under 100%, and power mismatches are minimal. No contingency violations are observed, indicating that the proposed plans maintain operational security even under single-element outages.

Table 4: Final AC N–1 validation.

System	$\lvert V \rvert$ dev. [p.u.]	Line loading [%]	Power mismatch [MW]	Violating cont. [#]
Legend: $a \to b$ means base-case value a and N–1 value b.				
RTS–24	0.006 → 0.018	92.0 → 99.0	0.6 → 2.1	0
IEEE–118	0.008 → 0.020	94.8 → 98.3	1.1 → 3.1	0
IEEE–300	0.010 → 0.024	95.6 → 99.2	2.6 → 6.4	0

4.4 Performance gains and solution quality

The proposed enhancements yield substantial computational benefits. The DFP reduces the number of exact SDP subproblem solves by approximately 75%, while the Magnanti–Wong (MW) strengthening accelerates convergence by reducing outer iterations. Despite these reductions, solution quality remains high: the final expansion plans achieve zero load shedding and pass full AC N–1 validation.

Numerical errors in AC feasibility checks remain within tight bounds—typically between 10^{-3} and 10^{-4}—consistent with the accuracy of the SDP relaxation and reliable recovery of rank-one solutions.

5 Conclusion

This work introduces a sequential planning framework that integrates a MILP master with SDP-relaxed AC OPF subproblems, enabling scalable and accurate transmission expansion planning under N–1 security constraints. By combining dual-feasible proxy cuts, Pareto-optimal strengthening, and adaptive contingency screening, the method achieves robust feasibility, accelerates convergence, and reduces computational burden. The framework supports multistage planning with full AC fidelity and demonstrates consistent performance across benchmark systems, achieving zero load shedding and tight feasibility margins.

The results show that the proposed model, integrating the $N - 1$ reliability criterion, ensures a reliable active and reactive power supply during contingencies for the expanded transmission network. Future research could focus on extending the proposed framework to integrate uncertainty related to renewable generation and demand using stochastic or robust formulations.

References

[1] I Alhamrouni, A Khairuddin, Ali Khorasani Ferdavani, and M Salem. Transmission expansion planning using ac-based differential evolution algorithm. IET Generation, Transmission & Distribution, 8(10):1637–1644, 2014.

[2] J Benders. Partitioning procedures for solving mixed-variables programming problems. Computational Management Science, 2(1), 2005.

[3] R Bent, G L Toole, and A Berscheid. Transmission network expansion planning with complex power flow models. IEEE Transactions on Power Systems, 27(2):904–912, 2011.

[4] X Fang, F Li, Y Wei, R Azim, and Y Xu. Reactive power planning under high penetration of wind energy using benders decomposition. IET Generation, Transmission & Distribution, 9(14):1835–1844, 2015.

[5] Elmira Fathipasandideh, Hussein Suprême, Hanane Dagdougui, and Dalal Asber. A novel sequential framework for transmission network expansion planning: Benders decomposition preceding semidefinite programming. In 2025 IEEE Kiel PowerTech, pages 1–6, 2025.

[6] B Ghaddar and R A Jabr. Power transmission network expansion planning: A semidefinite programming branch-and-bound approach. European Journal of Operational Research, 274(3):837–844, 2019.

[7] R A Jabr. Optimization of ac transmission system planning. IEEE Transactions on Power Systems, 28(3):2779–2787, 2013.

[8] Steven H Low. Convex relaxation of optimal power flow—part i: Formulations and equivalence. IEEE Transactions on Control of Network Systems, 1(1):15–27, 2014.

[9] S Lumbreras and R Andrés. The new challenges to transmission expansion planning. survey of recent practice and literature review. Electric Power Systems Research, 134:19–29, 2016.

[10] Leonardo H Macedo, Cristiam V Montes, John F Franco, Marcos J Rider, and Rubén Romero. Milp branch flow model for concurrent ac multistage transmission expansion and reactive power planning with security constraints. IET Generation, Transmission & Distribution, 10(12):3023–3032, 2016.

[11] Mahdi Mehrtash, Amin Kargarian, and Mohsen Rahmani. Security-constrained transmission expansion planning using linear sensitivity factors. IET Generation, Transmission & Distribution, 14(2):200–210, 2020.

[12] D K Molzahn, F Dörfler, H Sandberg, S H Low, S Chakrabarti, R Baldick, and J Lavaei. A survey of distributed optimization and control algorithms for electric power systems. IEEE Transactions on Smart Grid, 8(6):2941–2962, 2017.

[13] Saeed Peyghami, Pooya Davari, Mahmud Fotuhi-Firuzabad, and Frede Blaabjerg. Standard test systems for modern power system analysis: An overview. IEEE industrial electronics magazine, 13(4):86–105, 2019.

[14] Guancheng Qiu, Mathieu Tanneau, and Pascal Van Hentenryck. Dual conic proxy for semidefinite relaxation of ac optimal power flow. arXiv preprint arXiv:2502.06978, 2025.

[15] M J Rider, A V Garcia, and R Romero. Power system transmission network expansion planning using ac model. IET Generation, Transmission & Distribution, 1(5):731–742, 2007.

[16] L A Roald, D Pozo, A Papavasiliou, DK Molzahn, J Kazempour, and A Conejo. Power systems optimization under uncertainty: A review of methods and applications. Electric Power Systems Research, 214:108725, 2023.

[17] H Suprême, M de Montigny, N Compas, G Vanier, M M Dione, and N Qako. OSER – A planning tool for power systems operation simulation and for impacts evaluation of the distributed energy resources on the transmission system. IEEE Transactions on Smart Grid, 14(2):1103–1116, 2022.

[18] H Suprême, M de Montigny, M M Dione, O Ramos-Leaños, and N Compas. A quasi-static time-series approach to assess the impact of high distributed energy resources penetration on transmission system expansion planning. Electric Power Systems Research, 235:110635, 2024.

[19] Hussein Suprême, Martin de Montigny, and Nicolas Compas. A coordinative multi-stage techniques for reactive power management and transmission system voltage control for quasi-static time-series simulations. IEEE Transactions on Smart Grid, 2025. In review.

[20] H Wolkowicz, R Saigal, and L Vandenberghe. Handbook of semidefinite programming: theory, algorithms, and applications, volume 27. Springer Science & Business Media, 2012.